Report

Layer-Specific Entrainment of Gamma-Band Neural Activity by the Alpha Rhythm in Monkey Visual Cortex

Eelke Spaak,[1] Mathilde Bonnefond,[1] Alexander Maier,[2,3]
David A. Leopold,[2] and Ole Jensen[1,*]
[1]Donders Institute for Brain, Cognition, and Behaviour,
Radboud University Nijmegen, 6500 HE Nijmegen,
The Netherlands
[2]Section on Cognitive Neurophysiology and Imaging,
Laboratory of Neuropsychology, National Institute of Mental
Health, National Institutes of Health, Bethesda,
MD 20892, USA
[3]Department of Psychology, College of Arts and Science,
Vanderbilt University, Nashville, TN 37203, USA

Summary

Although the mammalian neocortex has a clear laminar organization, layer-specific neuronal computations remain to be uncovered. Several studies suggest that gamma band activity in primary visual cortex (V1) is produced in granular and superficial layers and is associated with the processing of visual input [1–3]. Oscillatory alpha band activity in deeper layers has been proposed to modulate neuronal excitability associated with changes in arousal and cognitive factors [4–7]. To investigate the layer-specific interplay between these two phenomena, we characterized the coupling between alpha and gamma band activity of the local field potential in V1 of the awake macaque. Using multicontact laminar electrodes to measure spontaneous signals simultaneously from all layers of V1, we found a robust coupling between alpha phase in the deeper layers and gamma amplitude in granular and superficial layers. Moreover, the power in the two frequency bands was anti-correlated. Taken together, these findings demonstrate robust interlaminar cross-frequency coupling in the visual cortex, supporting the view that neuronal activity in the alpha frequency range phasically modulates processing in the cortical microcircuit in a top-down manner [7].

Results

The laminar organization of the mammalian neocortex has been the subject of many anatomical studies [8, 9]. This work has revealed a layer-specific organization both within cortical columns and between brain areas including thalamic regions. To comprehend the functional role of this laminar organization, it is essential to uncover the dynamical interactions between layers. Neuronal oscillatory activity dominated in primary visual cortex (V1) by the alpha (7–14 Hz) and gamma (30–200 Hz) frequency bands has been demonstrated to be modulated during various types of processing and cognitive manipulations [2–7, 10]; however, the interactions between these frequency bands, and their laminar profile, remain poorly understood.

To better understand these interactions, we recorded spontaneous cortical activity from V1 of two awake, healthy adult

monkeys (*Macaca mulatta*) at rest using a 24-contact laminar electrode, which allowed us to simultaneously sample from all cortical layers (Figure 1A). Visual inspection of the local field potential (LFP) data revealed segments of high ongoing alpha activity amid segments with much less pronounced alpha (see Figure 1B for example), and parts of the analyses described here were restricted to such high-alpha segments (see Supplemental Experimental Procedures available online for details on the selection procedure). To minimize the contribution of volume conduction, we used locally bipolar LFP signals. The resulting mean power spectrum over all bipolar measurements during the high-alpha epochs is shown in Figure 1C. A peak in the alpha band (most strongly at 8 Hz) embedded in the 1/f power spectrum that characterizes electrophysiological measures of brain activity [11] is clearly visible.

Layer-Specific Entrainment of Gamma Power by the Phase of the Alpha Rhythm

We found that LFP power in the gamma band (30–200 Hz) was coupled to the phase of the alpha rhythm measured from electrodes in the infragranular layers. This was observed by aligning time-varying power in the LFP spectrum to peaks of the alpha rhythm in infragranular layers. Averaging a total of ~3,000 peak-aligned traces resulted in a characteristic wavelet shape (Figure 2D). The mean time-frequency representations (TFRs) of power aligned to the infragranular alpha peaks for the different layers demonstrated a clear coupling between the power in the 50–200 Hz range and the phase of the alpha rhythm (Figure 2). This modulation was most pronounced in the supragranular and granular layers, reaching nearly 20% (Figures 2A and 2B). The modulation was smallest in the infragranular layers (sign test of mean rectified TFR; supragranular versus infragranular: $p < 10^{-8}$; granular versus infragranular: $p < 10^{-9}$; supragranular versus granular: not significant) (Figure 2C), demonstrating that the coupling is not just within layer but involves interaction between different laminar compartments. This result cannot be attributed to the high-alpha selection procedure, because qualitatively similar results were obtained when using the entire data set (Figure S1).

Phase-Amplitude Coupling across Frequencies and Layers

In contrast to the analysis in the previous section, where the selection of a given frequency and electrode position might affect the observed coupling pattern, we next applied a data-driven approach in which all positions and frequencies were analyzed for phase-amplitude coupling. Figure 3A shows cross-frequency coupling of phase and amplitude [12], with the phase derived from the LFP signal in the infragranular layers and the amplitude measured from either the supragranular layers (upper panels) or granular layer (lower panels). Coupling was specific to gamma band amplitude locked to the phase in the alpha band ($p < 0.001$ to $p < 0.05$; cluster-based permutation test). In both monkeys, significant coupling was found in two separate gamma bands [13] (~30–70 and ~100–200 Hz). This division was most evident when considering infragranular phase and granular amplitude. It has been

*Correspondence: ole.jensen@donders.ru.nl

A

Macaque Primary
Visual Cortex

Surface
Supra-
granular
Granular
Infra-
granular
White matter

B

Gamma activity

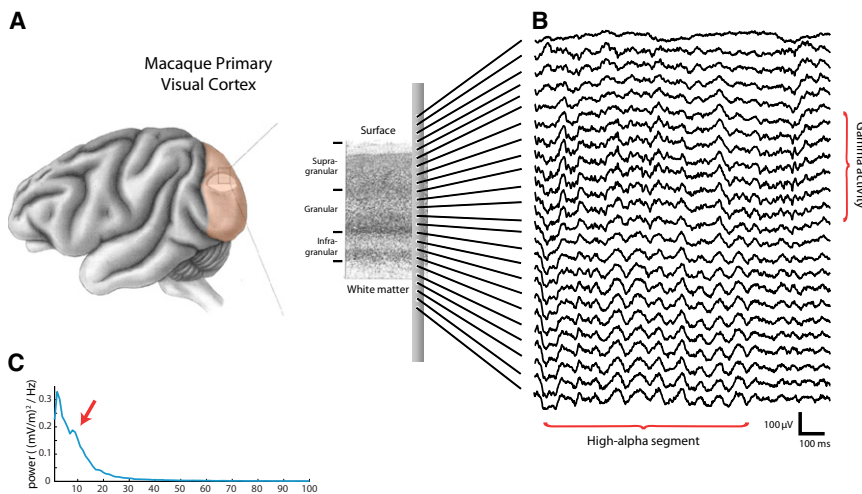100 μV

100 ms

High-alpha segment

C

Figure 1. Overview of the Type of Data We Acquired

(A) Continuous electrophysiological activity was simultaneously recorded from all layers of primary visual cortex using a 24-contact laminar probe in two monkeys.

(B) Example of the recorded voltage traces. The example traces show more prominent gamma activity in the superficial layers and a transient segment of alpha activity in the deep layers (about nine cycles).

(C) The power spectrum of bipolar data in infra-granular layers. Note the local peak in the alpha band, indicated by the arrow.

proposed that some of the power in the high gamma band (>100 Hz) can be explained by broadband contributions from spiking activity [14], whereas 30–70 Hz power is a consequence of oscillatory neuronal synchronization. In future work, it would be of interest to quantify the contribution from spiking to the high gamma band. This would require an independent measure of neuronal spiking, which the present data do not contain.

Figure 3B presents gamma amplitude binned as a function of alpha phase. Across the two monkeys, the gamma amplitude showed a phase modulation exceeding 10%, with somewhat stronger coupling in the granular than supragranular compartments. Note that this percent modulation is robust but somewhat smaller than that reported in Figure 2. The smaller modulation may be due to a lack of phase stationarity in the alpha band signal, leading to an effective decrease in the coupling magnitude.

To determine the laminar profile of the observed phase-amplitude coupling, we computed the alpha-to-gamma modulation index between all possible electrode combinations. Results for this analysis are shown in Figure 3C, where 0 is defined as the center of the granular layer [1, 15]. This plot reveals two well-circumscribed regions in which gamma amplitude was coupled to the infragranular alpha phase measured at -300 μm. One of these regions is located around 700 μm, in the supragranular layers (yellow arrow), whereas the other is located at around -300 μm (white arrow). Both regions were similar in the two monkeys. Note that given the bipolar referencing and the spatial separation of the two signals in the case of the supragranular region, the observed cross-frequency coupling cannot be due to an inherent broadband composition of either, or both, of the signals being compared.

Gamma Amplitude and Burst Duration Are Inversely Related to Alpha Amplitude

Consistent with the notion that alpha activity serves to inhibit neuronal processing [6, 7], we here report that alpha and gamma amplitude are inversely correlated. We investigated the correlation between the alpha and gamma amplitude on a 2 s, segment-by-segment basis. To control for nonphysiological signals producing spurious correlations, we used a partial correlation analysis controlling for the contribution from broadband (7–200 Hz) activity. We found significant

negative correlations between the alpha amplitude around -300 μm and the gamma amplitude either at that same location (monkey 1: $r_{\alpha\gamma \cdot broad} = -0.38$; monkey 2: $r_{\alpha\gamma \cdot broad} = -0.50$) or at 700 μm (monkey 1: $r_{\alpha\gamma \cdot broad} = -0.22$; monkey 2: $r_{\alpha\gamma \cdot broad} = -0.29$; all p < 0.001). (See Figure S2 for a similar analysis in which we estimated gamma amplitude separately for different alpha phases: we find a more negative correlation when gamma amplitude is estimated at the alpha troughs versus at the alpha peaks.)

Next we found that long gamma bursts were predominantly observed during periods of low alpha amplitude (see Figure S3). We detected gamma bursts (defined as 5–50 ms segments exceeding the 60th percentile of gamma amplitude) and computed the infragranular alpha amplitude in a 100 ms window around the bursts. The alpha and gamma amplitude time series were normalized by dividing both by the broadband (7–200 Hz) amplitude time series. In both monkeys, we found a weak but highly significant negative correlation between the length of a gamma burst and the alpha amplitude in a window around it (monkey 1: $r = -0.070$, $p < 10^{-5}$; monkey 2: $r = -0.067$, $p < 10^{-3}$).

Current Sources of Gamma-Coupled Alpha Rhythm Suggest an Infragranular Generator

To identify the generators of the alpha currents associated with the modulated gamma activity, we performed a current-source density (CSD) analysis [16]. We detected troughs in the alpha band in a supragranular unipolar electrode located at 700 μm. Around the alpha troughs, we averaged segments of LFP activity (Figure 4A) and estimated the CSD (Figure 4B). A clear alternating sink/source pattern can be observed straddling the granular/infragranular boundary. Also note the sink/source pattern in the supragranular domain.

Next we aimed to find the generators associated with the modulation of the superficial gamma activity by aligning the LFP traces to the incidences of gamma bursts. We first detected peaks in the gamma activity at the superficial unipolar electrode located at 700 μm (Figure 4C, black arrow). We then averaged epochs around these peaks. This analysis revealed a clear nesting of gamma bursts in the lower-frequency oscillation of the LFP (Figure 4C; superimposed blue lines indicate 7–14 Hz band-pass-filtered signals) [17].

The CSD of these traces revealed a prominent low-frequency sink in the granular layer coinciding with the gamma burst, accompanied by a source directly below (Figure 4D). Approximately 70 ms before and after the gamma burst, sinks were apparent in the infragranular layers (probably layer 5) and
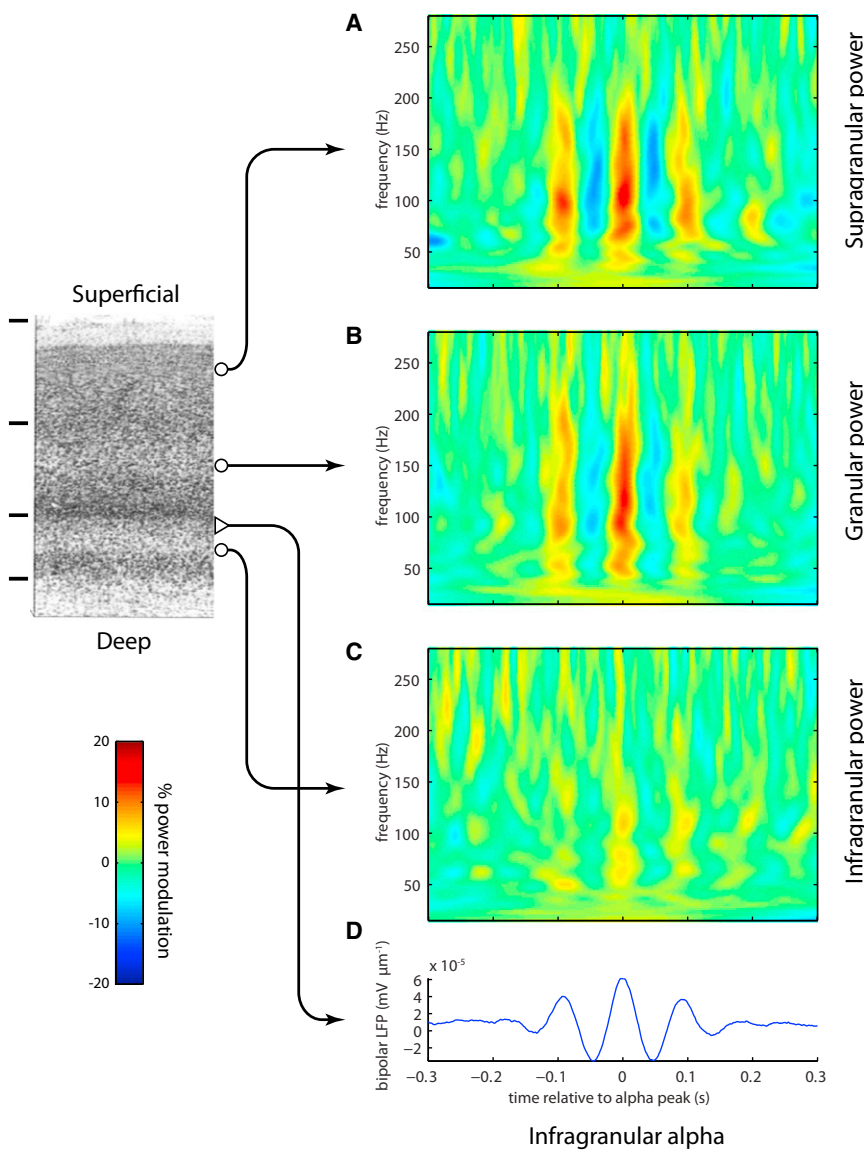
Figure 2. Time-Frequency Representations of Power for Epoch Time Locked to the Peaks of the Alpha Rhythm

TFRs were calculated per epoch and then averaged.

(A and B) The TFRs for the supragranular (A) and granular (B) layers reveal a robust modulation in the gamma activity (50–200 Hz) phase locked to the alpha oscillations.

(C) The modulation was virtually absent in the infragranular layers. The TFRs were normalized relative to the average power per frequency.

(D) The averaged unfiltered traces reveal alpha activity in the bipolar local field potential (LFP). The averaged TFRs and LFPs were calculated from ~3,000 epochs.

See Figure S1 for the same analysis conducted on all data, without preselection of high-alpha segments.

fluctuations in the alpha amplitude are inversely related to both the amplitude and burst length of the gamma activity.

In humans, it has been demonstrated that the phase of the alpha rhythm is predictive of perception [18–20], blood oxygen level-dependent responses [21], and gamma band activity [22, 23]. Laminar recordings in monkey have identified gamma generators in granular and supragranular layers [1] and alpha generators in deeper layers ([15, 24, 25]; T.J. van Kerkoerle et al., 2011, Soc. Neurosci., abstract) (albeit there is also evidence for supragranular alpha generators [25]). We now add to this body of work by revealing an intimate relationship between the neuronal dynamics in the alpha and gamma band: the alpha activity in deeper layers modulates the gamma band activity in granular and supragranular layers in a suppressive, phase-specific manner.

were accompanied by sources in the granular layer. Calculating the CSD aligned to gamma bursts measured from the granular layers yielded comparable results (Figure S4). The spatial distribution for the alpha-aligned current sources and sinks is highly similar to the sinks and sources we find when aligning to gamma bursts (compare Figure 4B and Figure 4D). However, note that the frequency for the alpha-aligned CSD is around 10 Hz, whereas the gamma burst-aligned CSD frequency is slightly lower. Overall, the laminar pattern of sinks and sources associated with the alpha rhythm and gamma bursts are highly consistent across both monkeys.

Discussion

Using laminar neurophysiological recordings, we have demonstrated that the amplitude of gamma activity (30–200 Hz) is coupled to the phase of alpha oscillations (7–14 Hz) within the V1 cortical microcircuit. This coupling is spatially specific: gamma activity in the granular and supragranular layers is coupled to the phase of alpha oscillations with generators extending to infragranular layers. Furthermore,

It bears emphasizing that most analyses were restricted to data segments exhibiting pronounced alpha activity, with "high-alpha" periods amounting to a small proportion of our extensive data set (approximately 3% using a conservative threshold; see Supplemental Experimental Procedures for details). In humans, the fraction of alpha rhythm in V1 during rest is considerably greater. We cannot rule out that the low fraction of alpha rhythm in both monkeys stemmed from active exploration of the room, though this seems unlikely given the absence of novel or interesting events. Comparing the prevalence of high-amplitude alpha rhythm in the macaque to that in humans would require a controlled, comparative study between the two species. In the present study, our results were qualitatively similar when we applied the analysis to the entire data set (e.g., Figures S1, S3, and S4), demonstrating that the coupling between frequencies is not only present during periods of high-amplitude alpha.

It should be noted that some of the effects we assign to the alpha band at 7–10 Hz overlaps with the theta frequency range. However, given that we study the visual system, that the generators were in the deeper layers of V1, and that the
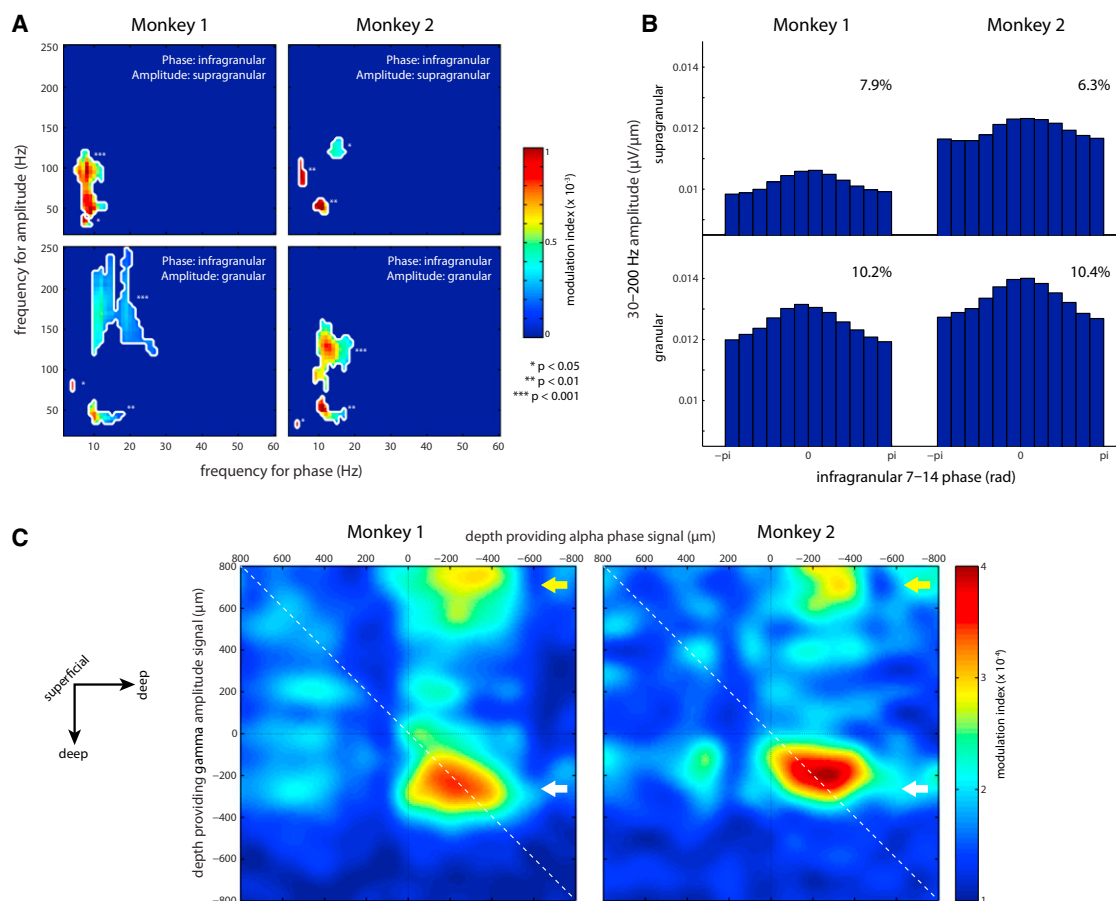
Figure 3. Modulation Index Analysis for Phase-Amplitude Coupling

(A) Modulation index (MI) values as shown for four representative bipolar channel pairs (each from a single recording session). Only significant MI values are shown. The significance values are corrected for multiple comparisons by a shift-predictor cluster permutation approach.

(B) Granular/supragranular gamma amplitude as a function of binned infragranular alpha phase, averaged over all recording sessions. The effect size of the modulation is shown above the graphs.

(C) Topographical representations of the alpha (7–14 Hz) to gamma (30–200 Hz) MI when considering all electrode combinations. The arrows indicate the deep-layer alpha phase modulation of the granular (white arrow) and supragranular (yellow arrow) gamma amplitude.

7–10 Hz activity correlated negatively with gamma amplitude, we deemed the term alpha to be appropriate. Nonetheless, for some of our analyses, coupling did extend well into the theta range and below (i.e., <8 Hz; see Figure 3A).

It has been proposed that neuronal synchronization in the gamma band, as observed for instance during visual processing [1–3], results in a stronger drive to downstream regions. Thus, modulating the degree of this synchronization might serve as a mechanism for feedforward gain control [26]. Indeed, when attention is allocated to a specific spatial location, visual stimuli elicit stronger gamma spike-field coherence in V4 neurons whose receptive fields correspond to that location [27]. Furthermore, in V1, V2, and V4, alpha synchrony in deep layers decreases with attention, whereas gamma synchrony in superficial layers increases [28]. Because alpha band activity is strongly modulated by spatial attention tasks—independently of whether there is visual stimulation present—and suppressed by visual input, this rhythm has been proposed to reflect top-down modulation of neuronal processing; specifically, it is thought to functionally inhibit sensory brain regions [4, 6, 7, 29].

Our results do not conclusively demonstrate the directionality of the coupling between alpha and gamma band activity:

although alpha activity could phasically modulate gamma activity, it is also conceivable that gamma activity has a causal impact on alpha phase instead. However, alpha is strongly modulated in a top-down manner even in the absence of visual input, in contrast to gamma activity, whose modulation is directly linked to the processing of visual stimuli. Therefore, we hypothesize a mechanism in which alpha activity modulates neuronal processing reflected in the gamma band and thus implements a mechanism for gain control. Such gain control might be implemented by regulating the duty cycle of processing within an alpha cycle. Strong alpha activity allows for only short bouts of processing to occur, whereas low alpha activity allows for longer bouts of processing (see Figure S2 and [7]).

Our CSD analysis of the ongoing alpha rhythm revealed sinks in the granular layer, co-occurring with sources in the infragranular layers (Figures 4B and 4D). Although it is difficult to pinpoint the precise basis for this pattern, one possibility would be that the zero-lag source is an active source corresponding to afterhyperpolarization currents in layer 5 (L5) cells [30]. However, a more conventional interpretation would be that the zero-lag sink is active. Although this sink might represent synchronized synaptic input to layer 4 neurons
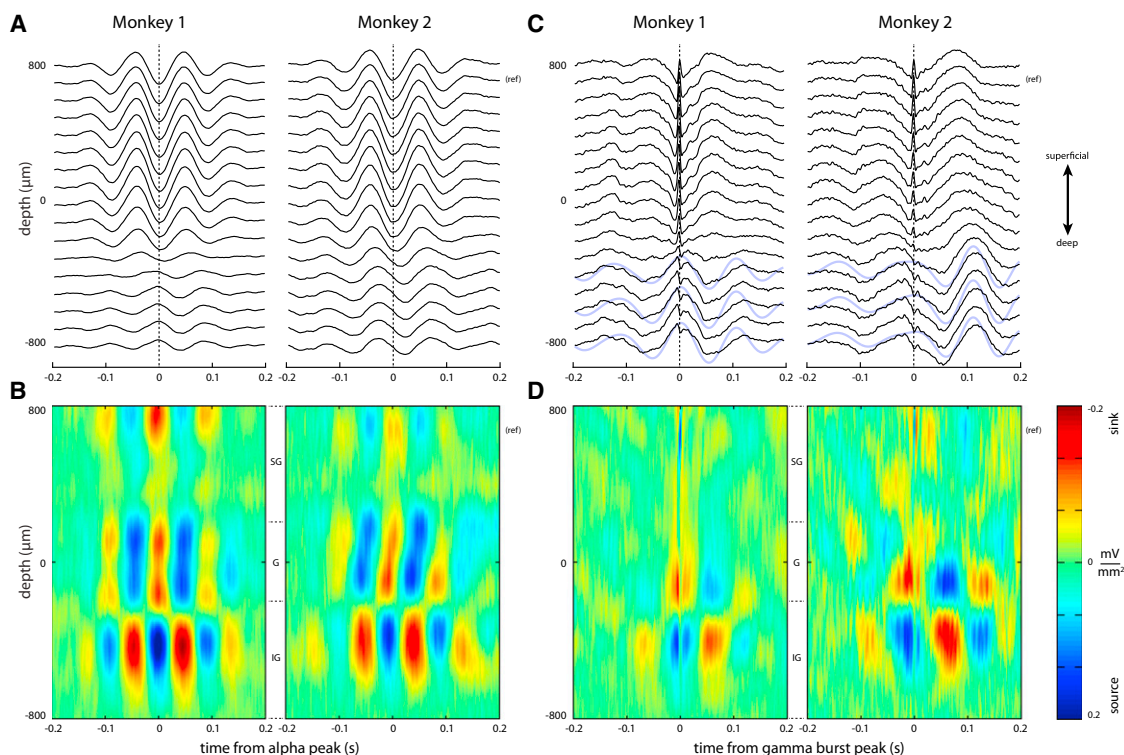
Figure 4. Laminar Activity Time Locked to Alpha Troughs or Gamma Bursts

(A) Average voltage traces phase locked to alpha troughs. The troughs were identified in the superficial layers [reference electrode indicated with "(ref)"].
(B) Current-source densities (CSDs) for the traces shown in (A).
(C) Average voltage traces phase locked to gamma bursts. The arrow on the right indicates the electrode used for identifying the gamma activity in superficial layers. In the raw averaged traces, a low-frequency profile emerges in the deep layers. Superimposed blue lines indicate 7–14 Hz band-pass-filtered signals for three infragranularly located electrodes.
(D) CSDs computed on the traces shown in (C). Alpha-frequency sink/source alternations are apparent around -100 and -400 μm.
See Figure S4 for voltage traces and CSD triggered to gamma bursts in the granular layer.

themselves, it could also arise from synapses on the proximal segment of L5 pyramidal cell apical dendrites [16], consistent with the involvement of infragranular neurons in the generation of the alpha rhythm [24]. Such synchronized input to L5 cells would likely be effective in bringing these cells above firing threshold [3, 31]. L5 pyramidal cells project to interneurons in the same layer [32, 33], which in turn project to the superficial layers [34–36]. This microanatomical pathway could explain how alpha oscillations exercise phasic inhibitory control over the gamma activity. Furthermore, this idea would be in line with recent findings demonstrating that cholinergic agonists concurrently enhance both attention and alpha activity [37]: L5 interneurons are specifically targeted by cholinergic afferents [38]. An alternative explanation for this intracolumnar route is that the deeper layers modulate gamma activity through a thalamic route. Electrophysiological studies have shown phase coherence between alpha activity in the lateral geniculate nucleus (LGN) of the thalamus and early visual cortices [39, 40]. Furthermore, infragranular layers are known to project to the LGN [9, 41]. Because the LGN projects to the granular layer in V1, which in turn projects to superficial layers, such a corticothalamocortical interaction might also explain the present findings. Future research combining anatomy with electrophysiological stimulation and measurements is required to determine whether the intracolumnar alpha-gamma coupling we observe is due to purely cortical anatomical connections or whether the thalamus is involved.

In conclusion, our findings are consistent with the notion that processing in the gamma band is clocked by slower rhythms [42, 43]. In future work, it would be of great interest to investigate how the interaction between alpha and gamma activity changes with attentional demands. Furthermore, it would be important to elucidate the physiological mechanisms implementing the cross-frequency interactions, as they are currently not well understood.

Experimental Procedures

All relevant aspects of the experimental procedures were approved by the Institutional Animal Care and Use Committee of the National Institute of Mental Health. Data analyses were performed using MATLAB R2011a (MathWorks) either with custom-written scripts or with the FieldTrip toolbox [44] (http://www.ru.nl/neuroimaging/fieldtrip/). For complete materials and methods, see Supplemental Experimental Procedures.

Supplemental Information

Supplemental Information includes four figures and Supplemental Experimental Procedures and can be found with this article online at http://dx.doi.org/10.1016/j.cub.2012.10.020.

Acknowledgments

References

1. Maier, A., Adams, G.K., Aura, C., and Leopold, D.A. (2010). Distinct superficial and deep laminar domains of activity in the visual cortex during rest and stimulation. Front. Syst. Neurosci. *4*, 31.

2. Jensen, O., Kaiser, J., and Lachaux, J.P. (2007). Human gamma-frequency oscillations associated with attention and memory. Trends Neurosci. *30*, 317–324.

3. Fries, P., Nikolić, D., and Singer, W. (2007). The gamma cycle. Trends Neurosci. *30*, 309–316.

4. Thut, G., and Miniussi, C. (2009). New insights into rhythmic brain activity from TMS-EEG studies. Trends Cogn. Sci. *13*, 182–189.

5. Sauseng, P., Klimesch, W., Heise, K.F., Gruber, W.R., Holz, E., Karim, A.A., Glennon, M., Gerloff, C., Birbaumer, N., and Hummel, F.C. (2009). Brain oscillatory substrates of visual short-term memory capacity. Curr. Biol. *19*, 1846–1852.

6. Klimesch, W., Sauseng, P., and Hanslmayr, S. (2007). EEG alpha oscillations: the inhibition-timing hypothesis. Brain Res. Brain Res. Rev. *53*, 63–88.

7. Jensen, O., Bonnefond, M., and VanRullen, R. (2012). An oscillatory mechanism for prioritizing salient unattended stimuli. Trends Cogn. Sci. *16*, 200–206.

8. Callaway, E.M. (2004). Feedforward, feedback and inhibitory connections in primate visual cortex. Neural Netw. *17*, 625–632.

9. Thomson, A.M., and Bannister, A.P. (2003). Interlaminar connections in the neocortex. Cereb. Cortex *13*, 5–14.

10. Tallon-Baudry, C., and Bertrand, O. (1999). Oscillatory gamma activity in humans and its role in object representation. Trends Cogn. Sci. *3*, 151–162.

11. Bédard, C., Kröger, H., and Destexhe, A. (2006). Does the 1/f frequency scaling of brain signals reflect self-organized critical states? Phys. Rev. Lett. *97*, 118102.

12. Tort, A.B.L., Komorowski, R., Eichenbaum, H., and Kopell, N. (2010). Measuring phase-amplitude coupling between neuronal oscillations of different frequencies. J. Neurophysiol. *104*, 1195–1210.

13. Colgin, L.L., Denninger, T., Fyhn, M., Hafting, T., Bonnevie, T., Jensen, O., Moser, M.-B., and Moser, E.I. (2009). Frequency of gamma oscillations routes flow of information in the hippocampus. Nature *462*, 353–357.

14. Belluscio, M.A., Mizuseki, K., Schmidt, R., Kempter, R., and Buzsáki, G. (2012). Cross-frequency phase-phase coupling between θ and γ oscillations in the hippocampus. J. Neurosci. *32*, 423–435.

15. Maier, A., Aura, C.J., and Leopold, D.A. (2011). Infragranular sources of sustained local field potential responses in macaque primary visual cortex. J. Neurosci. *31*, 1971–1980.

16. Mitzdorf, U. (1985). Current source-density method and application in cat cerebral cortex: investigation of evoked potentials and EEG phenomena. Physiol. Rev. *65*, 37–100.

17. Chrobak, J.J., and Buzsáki, G. (1998). Gamma oscillations in the entorhinal cortex of the freely behaving rat. J. Neurosci. *18*, 388–398.

18. Mathewson, K.E., Gratton, G., Fabiani, M., Beck, D.M., and Ro, T. (2009). To see or not to see: prestimulus α phase predicts visual awareness. J. Neurosci. *29*, 2725–2732.

19. Busch, N.A., Dubois, J., and VanRullen, R. (2009). The phase of ongoing EEG oscillations predicts visual perception. J. Neurosci. *29*, 7869–7876.

20. Dugué, L., Marque, P., and VanRullen, R. (2011). The phase of ongoing oscillations mediates the causal relation between brain excitation and visual perception. J. Neurosci. *31*, 11889–11893.

21. Scheeringa, R., Mazaheri, A., Bojak, I., Norris, D.G., and Kleinschmidt, A. (2011). Modulation of visually evoked cortical FMRI responses by phase of ongoing occipital alpha oscillations. J. Neurosci. *31*, 3813–3820.

22. Osipova, D., Hermes, D., and Jensen, O. (2008). Gamma power is phase-locked to posterior alpha activity. PLoS One *3*, e3990.

23. Voytek, B., Canolty, R.T., Shestyuk, A., Crone, N.E., Parvizi, J., and Knight, R.T. (2010). Shifts in gamma phase-amplitude coupling frequency from theta to alpha over posterior cortex during visual tasks. Front. Hum. Neurosci. *4*, 191.

24. Lopes Da Silva, F.H., and Storm Van Leeuwen, W. (1977). The cortical source of the alpha rhythm. Neurosci. Lett. *6*, 237–241.

25. Bollimunta, A., Mo, J., Schroeder, C.E., and Ding, M. (2011). Neuronal mechanisms and attentional modulation of corticothalamic α oscillations. J. Neurosci. *31*, 4935–4943.

26. Salinas, E., and Sejnowski, T.J. (2001). Correlated neuronal activity and the flow of neural information. Nat. Rev. Neurosci. *2*, 539–550.

27. Fries, P., Reynolds, J.H., Rorie, A.E., and Desimone, R. (2001). Modulation of oscillatory neuronal synchronization by selective visual attention. Science *291*, 1560–1563.

28. Buffalo, E.A., Fries, P., Landman, R., Buschman, T.J., and Desimone, R. (2011). Laminar differences in gamma and alpha coherence in the ventral stream. Proc. Natl. Acad. Sci. USA *108*, 11262–11267.

29. Haegens, S., Nácher, V., Luna, R., Romo, R., and Jensen, O. (2011). α-Oscillations in the monkey sensorimotor network influence discrimination performance by rhythmical inhibition of neuronal spiking. Proc. Natl. Acad. Sci. USA *108*, 19377–19382.

30. Wu, J., and Okada, Y.C. (1999). Roles of a potassium afterhyperpolarization current in generating neuromagnetic fields and field potentials in longitudinal CA3 slices of the guinea-pig. Clin. Neurophysiol. *110*, 1858–1867.

31. Bernander, Ö., Koch, C., and Usher, M. (1994). The effect of synchronized inputs at the single neuron level. Neural Comput. *6*, 622–641.

32. Kapfer, C., Glickfeld, L.L., Atallah, B.V., and Scanziani, M. (2007). Supralinear increase of recurrent inhibition during sparse activity in the somatosensory cortex. Nat. Neurosci. *10*, 743–753.

33. Silberberg, G., and Markram, H. (2007). Disynaptic inhibition between neocortical pyramidal cells mediated by Martinotti cells. Neuron *53*, 735–746.

34. Dantzker, J.L., and Callaway, E.M. (2000). Laminar sources of synaptic input to cortical inhibitory interneurons and pyramidal neurons. Nat. Neurosci. *3*, 701–707.

35. Xu, X., and Callaway, E.M. (2009). Laminar specificity of functional input to distinct types of inhibitory cortical neurons. J. Neurosci. *29*, 70–85.

36. Iurilli, G., Ghezzi, D., Olcese, U., Lassi, G., Nazzaro, C., Tonini, R., Tucci, V., Benfenati, F., and Medini, P. (2012). Sound-driven synaptic inhibition in primary visual cortex. Neuron *73*, 814–828.

37. Bauer, M., Kluge, C., Bach, D., Bradbury, D., Heinze, H.J., Dolan, R.J., and Driver, J. (2012). Cholinergic enhancement of visual attention and neural oscillations in the human brain. Curr. Biol. *22*, 397–402.

38. Xiang, Z., Huguenard, J.R., and Prince, D.A. (1998). Cholinergic switching within neocortical inhibitory networks. Science *281*, 985–988.

39. Lopes da Silva, F.H., Vos, J.E., Mooibroek, J., and Van Rotterdam, A. (1980). Relative contributions of intracortical and thalamo-cortical processes in the generation of alpha rhythms, revealed by partial coherence analysis. Electroencephalogr. Clin. Neurophysiol. *50*, 449–456.

40. Lorincz, M.L., Kékesi, K.A., Juhász, G., Crunelli, V., and Hughes, S.W. (2009). Temporal framing of thalamic relay-mode firing by phasic inhibition during the alpha rhythm. Neuron *63*, 683–696.

41. Saalmann, Y.B., and Kastner, S. (2011). Cognitive and perceptual functions of the visual thalamus. Neuron *71*, 209–223.

42. Lakatos, P., Shah, A.S., Knuth, K.H., Ulbert, I., Karmos, G., and Schroeder, C.E. (2005). An oscillatory hierarchy controlling neuronal excitability and stimulus processing in the auditory cortex. J. Neurophysiol. *94*, 1904–1911.

43. Buzsáki, G. (2006). Rhythms of the Brain (Oxford: Oxford University Press).

44. Oostenveld, R., Fries, P., Maris, E., and Schoffelen, J.M. (2011). FieldTrip: Open source software for advanced analysis of MEG, EEG, and invasive electrophysiological data. Comput. Intell. Neurosci. *2011*, 156869.